Title
Rocking Response of Anchored Blocks Under Pulse-Type Motions

Journal
Journal of Engineering Mechanics, 127(5)

Authors
Makris, Nicos
Zhang, Jian

Publication Date
2001

Peer reviewed

ROCKING RESPONSE OF ANCHORED BLOCKS UNDER PULSE-TYPE MOTIONS

By Nicos Makris,[1] Member, ASCE, and Jian Zhang[2]

ABSTRACT: This paper examines the transient rocking response of anchored blocks subjected to physically realizable horizontal pulse-type motion. Restrainers with elastic-brittle and elastic-plastic behavior are considered. Under one-sine pulse, anchored blocks can overturn with two distinct modes of overturning: (1) by exhibiting one impact; and (2) without exhibiting any impact. It is found that restrainers are more efficient in preventing overturning of small slender blocks subjected to low frequency pulses. This study uncovers that, although for most of the frequency range anchored blocks survive higher accelerations than free-standing blocks, there is a finite frequency range where the opposite happens. This paper examines this counterintuitive behavior and explains the destructive effect that increased strength and increased ductility of restrainers have on the rocking stability of rigid structures when excited by certain ground motions.

INTRODUCTION

The most common approach to prevent violent rocking of tall, slender rigid structures is the use of restrainers (hold-downs). Rocking restrainers can range from high-strength bolts and cables to wire-cable isolators, rubber bands, and other hysteretic elements including damping devices. Although the rocking response of free-standing blocks has been the subject of several investigators [see references Zhang and Makris (2001)], the rocking response of anchored blocks has received limited attention. Dimentberg et al. (1993), following a probabilistic approach, concluded that, under a white-noise excitation, anchored blocks with elastic restrainers are much more stable than free-standing blocks. Herein the rocking stability of anchored blocks is revisited following a deterministic approach and it is shown that there is a finite frequency range where the conclusion of Dimentberg et al. (1993) does not hold.

In this study the rocking response of an anchored block subjected to pulse-type motions is investigated in depth. It is found that restrainers are more efficient in preventing overturning of small slender blocks. Larger blocks overturn only without experiencing any impact, and in this case, the effect of restrainers is marginal even when their strength is as large as the weight of the rocking mass. The study uncovers that, although for most of the frequency range anchored blocks survive higher accelerations than free-standing blocks, there is a frequency range where the opposite happens. This counterintuitive behavior is the result of the way that inertia and gravity forces combine. It is shown that, under a one-sine (Type-A) pulse with frequency ω_p, a free-standing block with frequency parameter p has two modes of overturning: one with impact (mode 1) and one without impact (mode 2). The transition from mode 1 to mode 2 is sudden, and once ω_p/p is sufficiently large, a substantial increase in the acceleration amplitude of the one-sine pulse is needed to achieve overturning. When a block is anchored, the transition from mode 1 to mode 2 happens at slightly larger values of ω_p/p and this results in a finite frequency range in which a free-standing block survives acceleration levels that are capable of overturning the same block when it is anchored. Fig. 1 shows a schematic of the problem at hand in which the restoring element on each side of the block represents the combined stiffness of all the restrainers that are present at the edge of the block that uplifts. The restrainers considered in this paper have an elastic preyielding behavior and exhibit finite strength. Two idealizations for the mechanical behavior of the restrainers are considered. The first simple idealization is an elastic-brittle behavior. It assumes linear elastic behavior until the ultimate strength F_u is reached, and once the strength of the restrainers is exceeded, it fractures and the block continues to rock without enjoying any restoring force. It is assumed that the stiffness of the restrainer maintains a constant value K until the restrainer fractures, and subsequently, its stiffness and strength are zero. The second, more realistic idealization assumes an elastic-plastic behavior. The restrainer behaves linearly until the ultimate strength F_u is reached, and subsequently deforms plastically until the fracture displacement u_f is reached. Beyond that point, the restrainer fractures and the block continues to rock without enjoying any restoring or dissipative force. The case of the elastic-brittle behavior, although a subcase of the more general elastic-plastic behavior, is of particular interest, because at the limit of tall, slender blocks, one can formulate a linear solution that is used to validate some of the counterintuitive results presented in this paper.

ELASTIC-BRITTLE BEHAVIOR

Nonlinear Formulation

Fig. 2 (center) illustrates the moment-rotation relation that results from the presence of restrainers with elastic-brittle be-

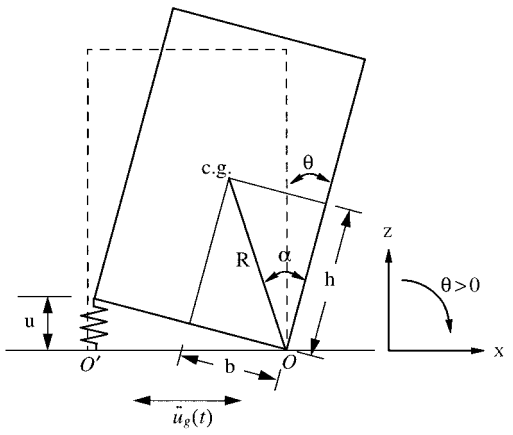

FIG. 1. Schematic of Anchored Block in Rocking Motion

[1]Assoc. Prof., Dept. of Civ. and Envir. Engrg., Univ. of California, Berkeley, CA 94720.

[2]Grad. Res. Asst., Dept. of Civ. and Envir. Engrg., SEMM, Univ. of California, Berkeley, CA 94720.

Note. Associate Editor: James Beck. Discussion open until October 1, 2001. Separate discussions should be submitted for the individual papers in this symposium. To extend the closing date one month, a written request must be filed with the ASCE Manager of Journals. The manuscript for this paper was submitted for review and possible publication on January 14, 2000; revised September 19, 2000. This paper is part of the ***Journal of Engineering Mechanics***, Vol. 127, No. 5, May, 2001. ©ASCE, ISSN 0733-9399/01/0005-0484–0493/$8.00 + $.50 per page. Paper No. 22197.

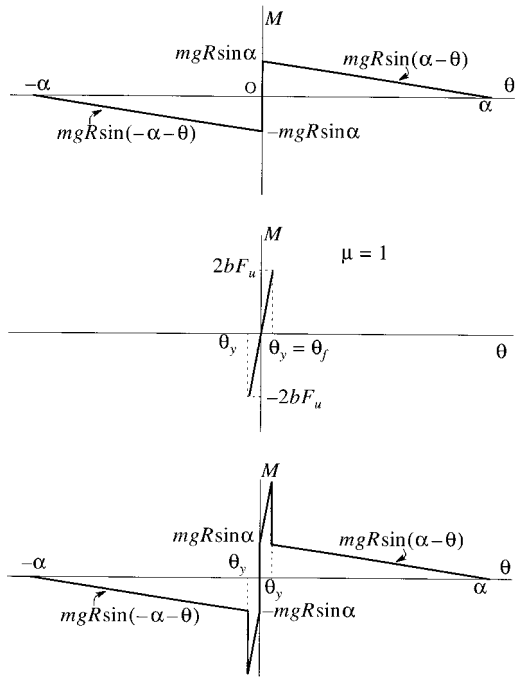

FIG. 2. Moment-Rotation Curves: (Top) Free-Standing Block; (Center) Elastic-Brittle Anchorage; (Bottom) Anchored Block with Elastic-Brittle Restrainers

havior, whereas Fig. 2 (top) illustrates the moment-rotation relation of a free-standing block. Under these two restoring mechanisms and assuming horizontal excitation alone, the equations that govern the rocking motion of an anchored block with mass m are

$$I_0\ddot{\theta}(t) + mgR\sin[-\alpha - \theta(t)] + 4Kb^2\sin\theta(t) = -m\ddot{u}_g(t)R\cos[-\alpha - \theta(t)], \quad \theta < 0 \tag{1}$$

$$I_0\ddot{\theta}(t) + mgR\sin[\alpha - \theta(t)] + 4Kb^2\sin\theta(t) = -m\ddot{u}_g(t)R\cos[\alpha - \theta(t)], \quad \theta > 0 \tag{2}$$

For a rectangular block, $I_0 = (4/3)mR^2$, (1) and (2) can be expressed in the compact form

$$\ddot{\theta}(t) = -p^2\left\{\sin(\alpha\ \mathrm{sgn}[\theta(t)] - \theta(t)) + \frac{3K\sin^2\alpha}{mp^2}\sin\theta(t) + \frac{\ddot{u}_g}{g}\cos[\alpha\ \mathrm{sgn}\,\theta(t) - \theta(t)]\right\} \tag{3}$$

in which $p = \sqrt{3g/(4R)}$.

Eq. (3) is valid as long as the restrainers hold. Once they fail, it reduces to

$$\ddot{\theta}(t) = -p^2\left\{\sin(\alpha\ \mathrm{sgn}[\theta(t)] - \theta(t)) + \frac{\ddot{u}_g}{g}\cos(\alpha\ \mathrm{sgn}\,\theta(t) - \theta(t))\right\} \tag{4}$$

which is the equation of motion of the free-standing block under horizontal excitation only [see Eq. (12) in Zhang and Makris (2001)].

Fig. 2 (bottom) shows the moment-rotation relation during the rocking motion of an anchored block. For rotation angles, $|\theta(t)| \le \theta_y$, energy is lost only during impact. Once θ_y is exceeded, the restrainer from the uplifted side fractures and additional energy is dissipated equal to the area of the small triangle that is superimposed on the moment-rotation graph of the free-standing block. This energy is dissipated once, because in subsequent postfracture oscillations, the moment-rotation relation reduces to that of the free-standing block.

The transition from (3) to (4) is conducted by following a fracture function $f(\theta)$. The finite ultimate strength of the restrainer F_u, in conjunction with the linear prefracture behavior, defines the angle of rotation θ_y that the restrainers yield and also, in this case, fracture

$$F_u = Ku_y = 2Kb\theta_y \tag{5}$$

from which

$$\theta_y = \frac{F_u}{2Kb} \tag{6}$$

The fracture function $f(\theta)$ is defined

$$f(\theta) = 1 \quad \text{when} \quad |\theta(t)| \le \theta_y \tag{7}$$

$$f(\theta) = 0 \quad \text{when} \quad |\theta(t)| \ge \theta_y \tag{8}$$

With the help of the fracture function, after replacing K/m with $(F_u/u_y)(g/W)$, the prefracture and postfracture equation of motion of the rigid block can be expressed in a compact form

$$\ddot{\theta}(t) = -p^2\left\{\sin[\alpha\ \mathrm{sgn}\,\theta - \theta(t)] + \frac{3F_u g\sin^2\alpha}{Wu_y p^2}\sin\theta(t)f(\theta) + \frac{\ddot{u}_g}{g}\cos[\alpha\ \mathrm{sgn}\,\theta - \theta(t)]\right\} \tag{9}$$

With this formulation, the rocking response of anchored blocks is described by four parameters: slenderness α, frequency parameter p (that includes the size effect), strength parameter $\sigma = F_u/W$; and influence factor $q = u_y p^2/g$. Table 1 summarizes the physical and mechanical parameters of selected electrical equipment utilized by Pacific Gas and Electric Co.

The solution of (9) is computed numerically by means of the state-space formulation introduced in Zhang and Makris (2001), where the state vector of the system is given by (48). The time-derivative vector $\mathbf{f}(t)$ is the one given by Eq. (49) in

TABLE 1. Geometrical, Physical, and Structural Parameters of Electrical Equipment

Equipment weight (kips)	b (in.)	h (in.)	K (kips/in.)	F_u (kips)	$\sigma = F_u/W$	α (degree)	p (rad/s)	$q = (u_y p^2)/g$	θ_y
40	36	84	175	4	0.100	23.20	1.7803	1.8×10^{-4}	5.56×10^{-4}
40	20	59	300	16	0.400	18.43	2.157	6.4×10^{-4}	1.33×10^{-3}
550	69	100	1,500	79	0.144	34.61	1.5441	3.2×10^{-4}	3.82×10^{-4}
193	38	89	1,000	53	0.275	23.12	1.7301	4.1×10^{-4}	6.97×10^{-4}
150	44	68	1,000	53	0.353	32.91	1.8911	4.9×10^{-4}	6.02×10^{-4}
230	38	90	1,500	79	0.343	22.89	1.7219	4.0×10^{-4}	6.93×10^{-4}
175	38	74	1,500	79	0.451	27.18	1.8660	4.7×10^{-4}	6.93×10^{-4}
60	35	90	500	26	0.433	21.25	1.7320	4.0×10^{-4}	7.43×10^{-4}
44	34	68	500	26	0.591	26.57	1.9519	5.7×10^{-4}	7.65×10^{-4}

Zhang and Makris (2001), in which its second component is replaced with the right-hand side of (9) of this paper.

This analysis concentrates on the overturning potential of a one-sine pulse shown in Fig. 4 (left) in Zhang and Makris (2001). Its ground acceleration is expressed

$$\ddot{u}_g(t) = a_p \sin(\omega_p t + \psi), \quad -\psi/\omega_p \le t \le (2\pi - \psi)/\omega_p \qquad (10a)$$

$$\ddot{u}_g(t) = 0, \quad \text{otherwise} \qquad (10b)$$

where $\psi = \sin^{-1}(\alpha g/a_p)$ = phase angle when rocking initiates.

Fig. 3 plots overturning acceleration spectra of a rigid block [$\alpha = 0.349$ rad (20°), $p = 2.0$ rad/s, and $\eta = \sqrt{r_{\max}} = 0.825$] under a one-sine pulse. The results are computed with the nonlinear formulation given by (9) for the case where $F_u/W = 0$ (free standing), $F_u/W = 0.4$, and $F_u/W = 1.0$. It is observed that anchored blocks have two modes of overturning following the same behavior that free-standing blocks exhibit. Overturning with mode 1 involves one impact, whereas overturning with mode 2 does not involve any impact. For small values of ω_p/p (say $\omega_p/p < 4$), anchored blocks survive higher accelerations; however, for values of $4 < \omega_p/p < 6$, anchored blocks topple under a lower acceleration than the acceleration needed to overturn the same block when it is free standing. This counterintuitive behavior happens in the neighborhood of the transition of mode 1 and mode 2. An anchored block enters this transition at a slightly larger value of ω_p/p. Furthermore, when a free-standing block has just entered mode 2 of overturning, the anchored block still overturns, because of mode 1 (overturning with impact), under a smaller acceleration amplitude. As ω_p/p increases, the anchored block will also overturn because of mode 2, and now a higher acceleration is needed to topple it in comparison to the acceleration needed to topple the free-standing block. However, the additional acceleration amplitude that an anchored block can withstand, even with $F_u/W = 1.0$, is negligible compared to the acceleration amplitude needed to overturn the free-standing block. Fig. 3 indicates that anchorages are effective at the low range of ω_p/p (low frequency pulses or small blocks or both).

Fig. 4 plots the ratio of the minimum acceleration needed to overturn an anchored block a_{p0}^{AN} to the minimum acceleration needed to overturn a free-standing block a_{p0}^{FS} for various values of the strength parameter $\sigma = F_u/W$. The results shown in Fig. 4 indicate that, under one-sine pulses with $\omega_p/p > 4$, blocks should not be anchored because the effect of restrainers is either destructive or virtually insignificant.

The limited capacity of the restrainers to prevent the toppling of a larger block is also illustrated by comparing the potential energy of the block at the verge of overturning with the strain energy dissipated by the restrainers.

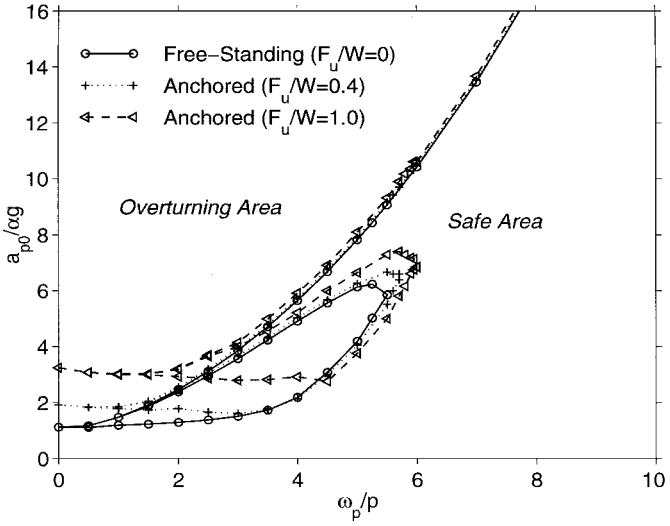

FIG. 3. Comparison of Overturning Acceleration Spectra due to One-Sine Pulse of Anchored Block ($\alpha = 0.349$ rad = 20°, $p = 2$ rad/s, $\eta = 0.825$, $q = 5.2 \times 10^{-4}$, and $\mu = 1$) Computed with Nonlinear Formulation

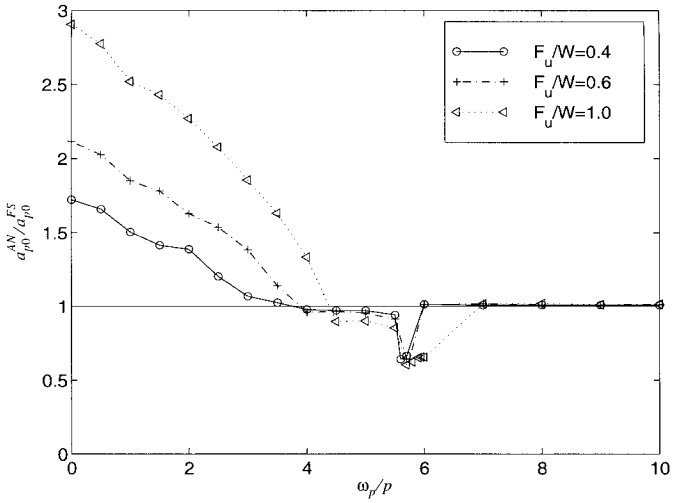

FIG. 4. Normalized Minimum Overturning Acceleration Levels Needed to Overturn Anchored Block (Elastic-Brittle Behavior, $\mu = 1$) to Acceleration Levels Needed to Overturn Same Block When It Is Free Standing

Assuming an elastic-brittle behavior, Fig. 2 (center) indicates that the strain energy dissipated by the restrainers before they fracture is

$$SE = \frac{1}{2} F_u u_y \qquad (11)$$

At the verge of overturning ($\theta = \alpha$), the kinetic energy of the block is zero because the one-sine pulse has expired and its potential energy is

$$PE = mgR(1 - \cos\alpha) \qquad (12)$$

The substitution of $\cos\alpha$ in (12) with its series expansion $1 - (\alpha^2/2) + \cdots$ gives

$$PE \approx mgR\frac{\alpha^2}{2} \qquad (13)$$

and the ratio of the dissipated strain energy to the total energy of the block at the verge of overturning is

$$\frac{SE}{PE} \approx \frac{F_u u_f}{mgR\alpha^2} = \frac{1}{\alpha^2}\frac{F_u}{W}\frac{u_y}{R} \qquad (14)$$

where $u_y = F_u/K$ = yield displacement. As an example, for a block with $\alpha = 0.349$ rad (20°), $p = 2.0$ rad/s, $R = 1.839$ m, $u_y = 1.25 \times 10^{-3}$ m, and $F_u = W$, the strain energy lost from the failure of each restrainer is approximately 0.6% of the energy that is needed to topple the free-standing block. Eq. (14) reveals some interesting geometrical and scale effects: (1) the $1/\alpha^2$ term indicates that restrainers are much more effective in preventing topping of the more slender of two blocks of the same size (same R); and (2) the $1/R$ term indicates that restrainers are more effective in preventing topping of the smaller of two geometrically similar blocks that have the same F_u/W.

Linear Formulation

Eqs. (1) and (2) and their compact form given by (9) are valid for arbitrary values of the block angle α. For slender blocks, the angle $\alpha = \tan^{-1}(b/h)$ is relatively small and (1) and (2) can be linearized. This linearization allows for the derivation of closed-form solutions when the excitation is ex-

pressed in a functional form. Herein, the solution of the linearized equations is derived for a sinusoidal ground motion for both positive and negative rotations to validate the fidelity of the numerical solution presented above. Within the limits of the linear approximation and for a ground acceleration

$$\ddot{u}_g(t) = a_p \sin(\omega_p t + \psi) \tag{15}$$

Eqs. (1) and (2) become

$$\ddot{\theta}(t) + \lambda^2 p^2 \theta(t) = -p^2 \frac{a_p}{g} \sin(\omega_p t + \psi) + \alpha p^2, \quad \theta < 0 \tag{16}$$

$$\ddot{\theta}(t) + \lambda^2 p^2 \theta(t) = -p^2 \frac{a_p}{g} \sin(\omega_p t + \psi) - \alpha p^2, \quad \theta > 0 \tag{17}$$

where $\psi = \sin^{-1}(\alpha g/a_p)$ = phase when rocking initiates and $\lambda^2 = 3(F_u/W)(g/u_y p^2)\sin^2\alpha - 1 = 3(\sigma/q)\sin^2\alpha - 1$. For typical anchorages of electrical equipment $\lambda^2 > 0$. Once the restrainers fail, $\lambda^2 = -1$. Accordingly, the solution of (16) and (17) is presented for the four segments $-\theta_y \le \theta(t) \le 0$, $\theta(t) < -\theta_y \le 0$, $0 < \theta(t) < \theta_y$, and $0 < \theta_y < \theta(t)$

$$\theta(t) = A_1 \sin(\lambda p t) + A_2 \cos(\lambda p t) + \frac{\alpha}{\lambda^2} - \frac{1}{\lambda^2 - \frac{\omega_p^2}{p^2}} \frac{a_p}{g} \sin(\omega_p t + \psi_1),$$

$$-\theta_y \le \theta(t) \le 0 \tag{18}$$

$$\theta(t) = A_3 \sinh(pt) + A_4 \cosh(pt) - \alpha + \frac{1}{1 + \frac{\omega_p^2}{p^2}} \frac{a_p}{g} \sin(\omega_p t + \psi_2),$$

$$\theta(t) < -\theta_y \le 0 \tag{19}$$

$$\theta(t) = A_5 \sin(\lambda p t) + A_6 \cos(\lambda p t) - \frac{\alpha}{\lambda^2} - \frac{1}{\lambda^2 - \frac{\omega_p^2}{p^2}} \frac{a_p}{g} \sin(\omega_p t + \psi_3),$$

$$0 < \theta(t) < \theta_y \tag{20}$$

$$\theta(t) = A_7 \sinh(pt) + A_8 \cosh(pt) + \alpha + \frac{1}{1 + \frac{\omega_p^2}{p^2}} \frac{a_p}{g} \sin(\omega_p t + \psi_4),$$

$$0 < \theta_y < \theta(t) \tag{21}$$

where

$$A_1 = \frac{\dot{\theta}_0}{\lambda p} + \frac{1}{\lambda} \frac{\omega_p/p}{\lambda^2 - \omega_p^2/p^2} \frac{a_p}{g} \cos\psi_1 \tag{22}$$

$$A_2 = -\frac{\alpha}{\lambda^2} + \frac{1}{\lambda^2 - \omega_p^2/p^2} \frac{a_p}{g} \sin\psi_1 \tag{23}$$

$$A_3 = \frac{\dot{\theta}_y^-}{p} - \frac{\omega_p/p}{1 + \omega_p^2/p^2} \frac{a_p}{g} \cos\psi_2 \tag{24}$$

$$A_4 = -\theta_y + \alpha - \frac{1}{1 + \omega_p^2/p^2} \frac{a_p}{g} \sin\psi_2 \tag{25}$$

$$A_5 = \frac{\dot{\theta}_0}{\lambda p} + \frac{1}{\lambda} \frac{\omega_p/p}{\lambda^2 - \omega_p^2/p^2} \frac{a_p}{g} \cos\psi_3 \tag{26}$$

$$A_6 = \frac{\alpha}{\lambda^2} + \frac{1}{\lambda^2 - \omega_p^2/p^2} \frac{a_p}{g} \sin\psi_3 \tag{27}$$

$$A_7 = \frac{\dot{\theta}_y^+}{p} - \frac{\omega_p/p}{1 + \omega_p^2/p^2} \frac{a_p}{g} \cos\psi_4 \tag{28}$$

$$A_8 = \theta_y - \alpha - \frac{1}{1 + \omega_p^2/p^2} \frac{a_p}{g} \sin\psi_4 \tag{29}$$

In (22) and (23) $\psi_1 = \psi = \sin^{-1}(\alpha g/a_p)$ = phase when rocking initiates. In (24) and (25) $\psi_2 = \omega_p t_y^- + \psi$, where t_y^- is the time that $-\theta_y$ is reached. In (26) and (27), $\psi_3 = \omega_p t_i + \psi$, where t_i is the time when $\theta = 0$ and the block experiences its first impact. In (28) and (29), $\psi_4 = \omega_p t_y^+ + \psi$, where t_y^+ is the time that θ_y is reached. Stepping through time, the values of t_y^-, t_i, and t_y^+ are detected by monitoring the value of the rotation angle θ. The solution obtained with the linear formulation is used to validate the fidelity of the numerical solution of (9) that is achieved with a state-space formulation.

Fig. 5 plots the minimum overturning acceleration spectra of a rigid block ($\alpha = 0.349$ rad = 20°, $p = 2$ rad/s, and $\eta = 0.825$) with elastic-brittle restrainers under one-sine pulse, computed with the linear formula. A behavior similar to that computed with the nonlinear formulation is observed. For small values of ω_p/p (approximately $\omega_p/p < 4$), anchored blocks survive higher accelerations; however, for values of $\omega_p/p > 4$, anchored blocks topple under a lower acceleration than what is needed to overturn the same block when it is free standing. The results are computed with the analytical solution presented herein and the numerical integration that is achieved with a state-space formulation. The agreement of the two solutions is excellent.

The elastic-brittle behavior in conjunction with the linear formulation allows for an analytical solution that was used to validate the fidelity of the numerical integration. It was found that even at the limit of the linear approximation, there is a range of ω_p/p where a free-standing block can survive a stronger acceleration than when it is anchored. Fig. 6 compares the overturning spectra of an anchored block ($\alpha = 0.349$ rad = 20°, $p = 2$ rad/s, and $\eta = 0.825$) with $F_u/W = 0.4$ (top) and $F_u/W = 0.6$ (bottom) computed with the linear and nonlinear formulation. When the frequency of the one-sine pulse is relatively low, both formulations yield comparable results. As the excitation frequency increases, the linear formulation yields minimum overturning acceleration amplitudes drastically larger than those obtained with the nonlinear formulation. This result is because, under the nonlinear formulation, the overturning ''bay'' generated by mode 1 of overturning penetrates further into the safe area under the overturning spectrum due to mode 2. As the excitation frequency further increases, the linear and nonlinear formulations again yield comparable results. This finding indicates that, when $4 < \omega_p/p < 6$, the linear

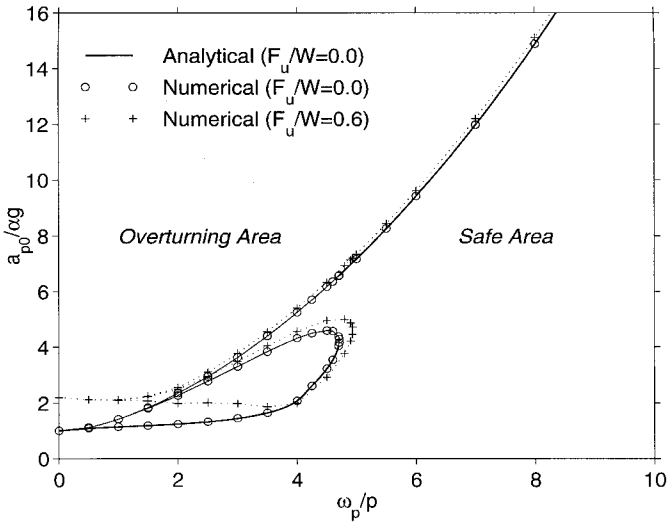

FIG. 5. Comparison of Overturning Acceleration Spectra due to One-Sine Pulse of Anchored Block ($\alpha = 0.349$ rad = 20°, $p = 2$ rad/s, $\eta = 0.825$, $q = 5.2 \times 10^{-4}$, and $\mu = 1$) Computed with Linear Formulation

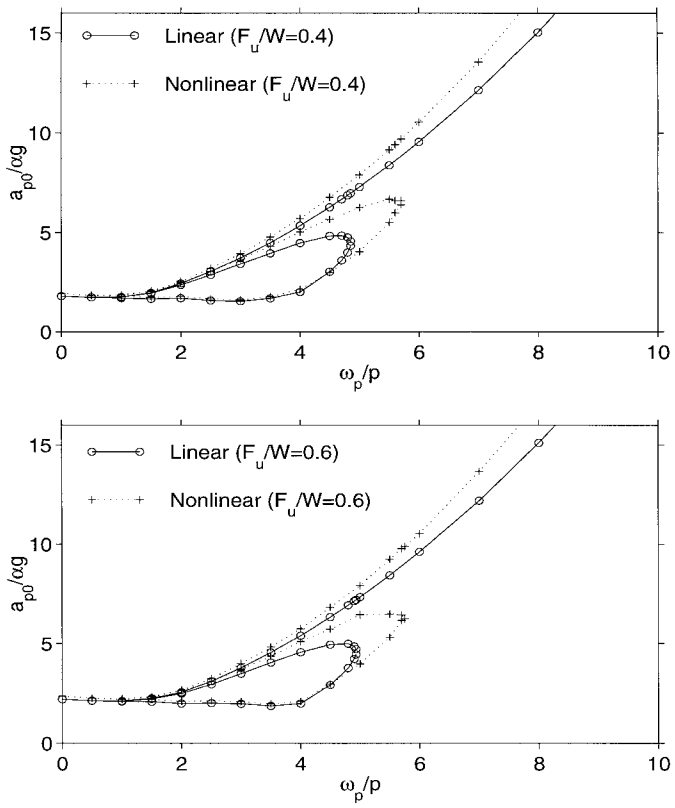

FIG. 6. Comparison of Overturning Acceleration Spectra due to One-Sine Pulse of Anchored Block ($\alpha = 0.349$ rad = 20°, $p = 2$ rad/s, $\eta = 0.825$, $q = 5.2 \times 10^{-4}$, and $\mu = 1$) Computed with Linear and Nonlinear Formulation for $F_u/W = 0.4$ (Top) and $F_u/W = 0.6$ (Bottom)

formulation should be avoided because it gives erroneous results even for slender blocks.

ELASTIC-PLASTIC BEHAVIOR

Fig. 7 illustrates the force-displacement relation of restrainers with ductile behavior. In general, the restrainers can exhibit a postyielding stiffness and maintain their strength until they reach a fracture displacement u_f. A measure of their ductile behavior is the ductility coefficient $\mu = u_f/u_y$. A suitable model to approximate such nonlinear hysteretic behavior is given by

$$P(t) = \varepsilon K u(t) + (1 - \varepsilon) K u_y Z(t) \tag{30}$$

where $u(t)$ = extension of the restrainer; K = preyielding stiffness; ε = ratio of the postyielding to preyielding stiffness; u_y = yield displacement; and $Z(t)$ = hysteretic dimensionless quantity that is governed by

$$u_y \dot{Z}(t) + \gamma |\dot{u}(t)| Z(t) |Z(t)|^{n-1} + \beta \dot{Z}(t) |Z(t)|^n - \dot{u}(t) = 0 \tag{31}$$

In the above equation β, γ, and n = dimensionless quantities that control the shape of the hysteretic loop. The hysteretic model, expressed by (30) and (31), was originally proposed by Bouc (1971) for $n = 1$, subsequently extended by Wen (1975, 1976), and used in random vibration studies of inelastic systems.

In this study, the special case of elastoplastic behavior is considered by setting the postyielding stiffness equal to zero ($\varepsilon = 0$). However, the developed formulation can easily be extended to account for situations with $\varepsilon \neq 0$.

Fig. 8 (center) illustrates the moment-rotation relation that results from the presence of restrainers with elastoplastic behavior, whereas Fig. 8 (top) illustrates again the moment-rotation relation of a free-standing block. Under these two restoring mechanisms, the equations that govern the rocking motion of an anchored block with mass m and moment of inertia I_0 (about pivot point O or O') is

$$I_0 \ddot{\theta}(t) + m\ddot{u}_g R \cos(-\alpha - \theta) = -mgR \sin(-\alpha - \theta) - P(t) 2b \cos\left(\frac{\theta}{2}\right), \quad \theta < 0 \tag{32}$$

$$I_0 \ddot{\theta}(t) + m\ddot{u}_g R \cos(\alpha - \theta) = -mgR \sin(\alpha - \theta) - P(t) 2b \cos\left(\frac{\theta}{2}\right), \quad \theta > 0 \tag{33}$$

where $P(t)$ = force originating from the restrainers, which for the general case is given by (30), and the special elastoplastic case ($\varepsilon = 0$) reduces to

$$P(t) = K u_y Z(t) \tag{34}$$

With reference to Fig. 8, $u_y = 2b\theta_y$ and (34) gives

$$P(t) = 2Kb\theta_y Z(t) \tag{35}$$

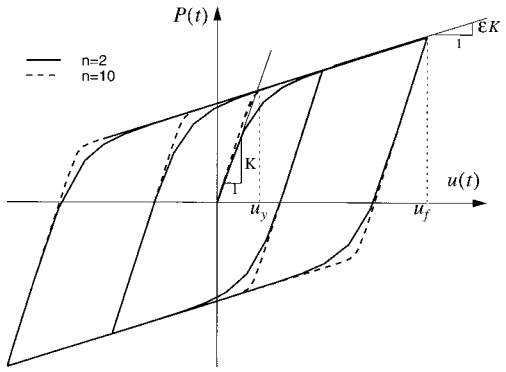

FIG. 7. Force-Displacement Curve of Element with Bilinear Behavior

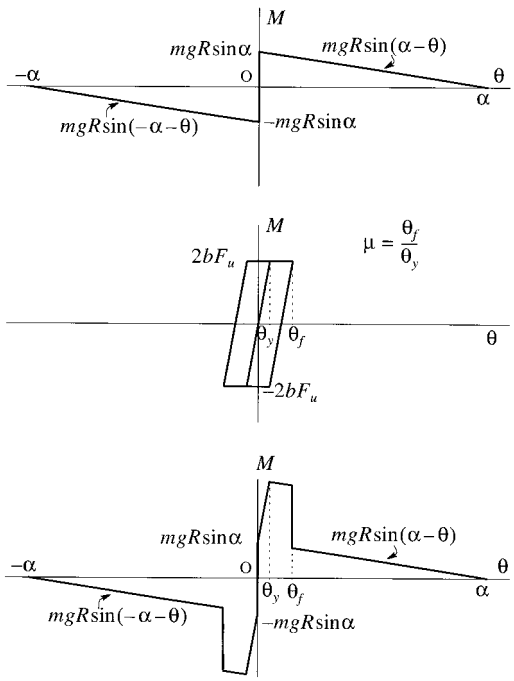

FIG. 8. Moment-Rotation Curves: (Top) Free-Standing Block; (Center) Elastic-Plastic Anchorage; (Bottom) Anchored Block with Elastic-Plastic Restrainers

Substitution of (35) into (32) and (33) gives

$$I_0\ddot{\theta}(t) + mgR\sin(-\alpha - \theta) + 4Kb^2\theta_y Z(t)\cos\left(\frac{\theta}{2}\right) = -m\ddot{u}_g(t)R\cos(-\alpha - \theta), \quad \theta < 0 \tag{36}$$

$$I_0\ddot{\theta}(t) + mgR\sin(\alpha - \theta) + 4Kb^2\theta_y Z(t)\cos\left(\frac{\theta}{2}\right) = -m\ddot{u}_g(t)R\cos(\alpha - \theta), \quad \theta > 0 \tag{37}$$

Using that for a rectangular block, $I_0 = (4/3)mR^2$, (36) and (37) can be expressed in the compact form

$$\ddot{\theta}(t) = -p^2\left\{\sin[\alpha\ \mathrm{sgn}\ \theta(t) - \theta(t)] + \frac{\ddot{u}_g(t)}{g}\cos[\alpha\ \mathrm{sgn}\ \theta(t) - \theta(t)] + \frac{3\sigma\sin^2\alpha}{q}\theta_y Z(t)\cos\left(\frac{\theta}{2}\right)\right\} \tag{38}$$

where $p = \sqrt{3g/(4R)}$; $\sigma = F_u/W$; $q = u_y p^2/g$; and $Z(t)$ = solution of (31), which in terms of rotations takes the form

$$\theta_y\dot{Z}(t) + \gamma|\dot{\theta}(t)|Z(t)|Z(t)|^{n-1} + \beta\dot{\theta}(t)|Z(t)|^n - \dot{\theta}(t) = 0 \tag{39}$$

Eq. (38) is valid as long as the restrainers hold. Once their fracture displacement, $u_f = 2b\sin\theta_f$, is reached, they do not provide any resistance and (38) reduces to the equation of motion of the free-standing block given by (4).

Fig. 8 (bottom) shows the moment-rotation relation during the rocking motion of an anchored block where its restrainers exhibit elastoplastic behavior. For rotation angles $|\theta(t)| \le \theta_y$, energy is lost only during the reversal of motion due to impact. Once θ_y is exceeded, the restrainers along the uplifted side yield. In the case where the motion reverses before the rotation reaches θ_f, additional energy is dissipated equal to the area of the flag-shaped shaded regions. This dissipation mechanism will be repeated as long as the maximum rotation does not reach the fracture rotation θ_f. If θ_f is exceeded, the restrainers fracture and the moment curvature curve reduces to that of the free-standing block.

The transition from (38) to (4) is conducted with the fracture function $f(\theta)$ defined

$$f(\theta) = 1 \quad \text{when} \quad |\theta(t)| \le \theta_f \tag{40}$$

$$f(\theta) = 0 \quad \text{when} \quad |\theta(t)| \ge \theta_f \tag{41}$$

where $\theta_f = \mu\theta_y$; and θ_y is given by (6). With the help of the fracture function, the prefracture and postfracture equation of rocking motion can be expressed

$$\ddot{\theta}(t) = -p^2\left\{\sin[\alpha\ \mathrm{sgn}\ \theta - \theta(t)] + \frac{\ddot{u}_g(t)}{g}\cos[\alpha\ \mathrm{sgn}\ \theta - \theta(t)] + \frac{3\sigma\sin^2\alpha}{q}\theta_y Z(t)\cos\left(\frac{\theta(t)}{2}\right)f(\theta)\right\} \tag{42}$$

The integration of (42) requires the simultaneous integration of (39). In this case the state vector of the system is

$$\{y(t)\} = \begin{Bmatrix}\theta(t)\\ \dot{\theta}(t)\\ Z(t)\end{Bmatrix} \tag{43}$$

and the time derivative vector $\mathbf{f}(t)$ is

$$\mathbf{f}(t) = \begin{Bmatrix}\dot{\theta}(t)\\ -p^2\left(\sin[\alpha\ \mathrm{sgn}\ \theta(t) - \theta(t)] + \frac{\ddot{u}_g}{g}\cos[\alpha\ \mathrm{sgn}\ \theta(t) - \theta(t)] + \frac{3\sigma\sin^2\alpha}{q}\theta_y Z(t)\cos\left(\frac{\theta(t)}{2}\right)f(\theta)\right)\\ \frac{1}{\theta_y}\left[\dot{\theta}(t) - \gamma|\dot{\theta}(t)|Z(t)|Z(t)|^{n-1} - \beta\dot{\theta}(t)|Z(t)|^n\right]\end{Bmatrix} \tag{44}$$

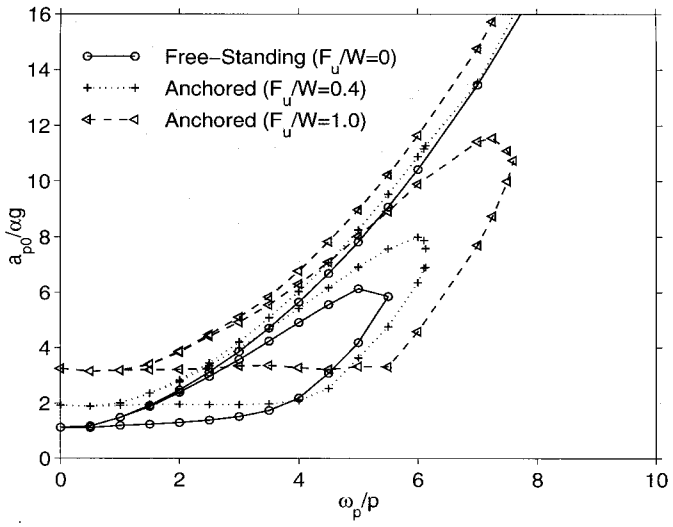

FIG. 9. Overturning Acceleration Spectra due to One-Sine Pulse of Anchored Block (α = 0.349 rad = 20°, p = 2 rad/s, η = 0.825, q = 5.2 $\times$ 10^{-4}, and μ = 5) Computed with Nonlinear Formulation

Fig. 9 plots the normalized minimum acceleration amplitude, $a_{p0}/\alpha g$, of a one-sine pulse needed to overturn an anchored block (α = 0.349 rad = 20°, p = 2 rad/s, and η = 0.825). The results are computed with the nonlinear formulation for an influence factor $q = 5.2 \times 10^{-4}$, ductility $\mu = 5$, and various values of the restrainer strength F_u/W.

At the zero limit of ω_p/p, a block with finite size is subjected to a very long duration pulse. When this pulse is near its peak, the block is subjected to a nearly constant acceleration a_{p0}. When the restrainers yield elastic-plastic behavior (Fig. 8), the balance of moment when the restrainers reach their ultimate strength is

$$ma_{p0}R\cos(\alpha - \theta_y) = mg\sin(\alpha - \theta_y) + F_u 2b\cos\left(\frac{\theta_y}{2}\right) \tag{45}$$

in which θ_y is given by (6). After dividing both sides of (45) with $mR\cos(\alpha - \theta_y)$, one obtains

$$a_{p0} = g\frac{\sin(\alpha - \theta_y)}{\cos(\alpha - \theta_y)} + 2\frac{F_u}{W}g\tan\alpha\frac{\cos(\theta_y/2)}{\cos(\alpha - \theta_y)} \tag{46}$$

Eq. (46) is the equivalent West's formula (Milne 1885) for an anchored block with elastoplastic restrainers that exhibit ultimate strength F_u. The parameters F_u, K, and b, related to electrical equipment, yield a value of θ_y much smaller than α, whereas $\cos(\theta_y/2) \approx 1$. Under these conditions (46) simplifies to

$$a_{p0} = g\tan\alpha + 2\frac{F_u}{W}g\tan\alpha\frac{1}{\cos\alpha} \tag{47}$$

and for slender blocks, $\tan\alpha \approx \alpha + \alpha^2/3$ and $\cos\alpha \approx 1 - \alpha^2/2$; therefore, (47) further simplifies to

$$\frac{a_{p0}}{\alpha g} \approx \left[1 + 2\frac{F_u}{W} + \alpha^2\left(\frac{1}{3} + \frac{5}{3}\frac{F_u}{W}\right)\right] \tag{48}$$

when terms are retained up to α^2.

At the zero-frequency limit, the numerical solution for a_{p0} approaches the static limit computed with (47) or with its slender-block approximation given by (48). As the ratio ω_p/p increases, the acceleration needed to overturn an anchored block with ductility $\mu = 5$ maintains a nearly constant value and then increases drastically. The larger the strength ratio, $\sigma = F_u/W$, the larger is the frequency range that the minimum overturning acceleration is constant. This finding leads to the counterintuitive situation, where within the range $4 < \omega_p/p < 7.5$, the stronger the restrainers, the smaller the acceleration needed to overturn the block; whereas, free-standing blocks are the most stable. When ω_p/p is sufficiently large so that an anchored block overturns with mode 2, an anchored block can sustain a slightly larger acceleration than free-standing blocks.

Fig. 10 plots the ratio between the minimum overturning acceleration of an anchored block a_{p0}^{AN} to the minimum overturning acceleration a_{p0}^{FS} of a free-standing block. In the frequency range, $4 < \omega_p/p < 7.5$, the ratio $a_{p0}^{AN}/a_{p0}^{FS} < 1$; therefore, the effect of anchorage is destructive. For an electrical equipment with frequency parameter $p \approx 2$ rad/s, this range corresponds to frequencies 1.27 Hz $< f_p <$ 2.28 Hz; or in terms of predominant pulse periods, 0.4 s $< T_p <$ 0.8 s. For this period range, which is of central interest to earthquake engineering, a free-standing block can withstand a larger acceleration amplitude than an anchored block.

Fig. 11 compares the overturning acceleration spectra of an anchored block ($\alpha = 0.349$ rad = 20°, $p = 2$ rad/s, and $\eta = 0.825$) that has restrainers with the same strength but different ductility. Again there is a frequency range where the block equipped with the less ductile restrainers will survive stronger accelerations than the block with more ductile restrainers.

The limited capacity of the restrainers with finite ductility to prevent the toppling of large blocks can be illustrated again by comparing the potential energy of the block at the verge of overturning with the strain energy dissipated by the ductile restrainers. Assuming an elastoplastic behavior ($\varepsilon = 0$), Fig. 8 (center) indicates that the strain energy dissipated by the restrainers before they fracture is

$$SE \approx F_u u_f \tag{49}$$

At the verge of overturning ($\theta = \alpha$), the kinetic energy of the block is zero because the one-sine pulse has expired and its potential energy is given by (13). Therefore, the ratio of the dissipated strain energy to the total energy of the block at the verge of overturning is

$$\frac{SE}{PE} \approx \frac{2F_u u_f}{mgR\alpha^2} = \frac{2}{\alpha^2}\frac{F_u}{W}\mu\frac{u_y}{R} \tag{50}$$

where $u_y = F_u/K$ = yield displacement.

For a value of $F_u/W = 1.0$ and ductility $\mu = 5$, the ratio SE/PE for the 0.5 × 1.5 m block ($\alpha = 0.3217$, $u_y = 1.30 \times 10^{-3}$ m, and $R = 1.581$ m) is equal to 8%, which is still a small fraction.

Eq. (50) reveals the same geometrical and scale effects: (1) the $1/\alpha^2$ term indicates that restrainers are much more effective in preventing toppling of the more slender of two blocks of the same size (same R); and (2) the $1/R$ term indicates that restrainers are more effective in preventing topping of the smaller of two geometrically similar blocks that have the same F_u/W.

Eq. (50) is the result of an ultimate strength approach that is independent of the dynamic effect. Consequently the ratio $(PE + SE)/PE$, which is the ratio of the total energy that the anchored block has adopted at the verge of overturning to the corresponding energy that the free-standing block has adopted, does not relate directly to the ratio between the minimum overturning acceleration of the anchored block a_{p0}^{AN} and the minimum overturning acceleration a_{p0}^{FS} of the free-standing block.

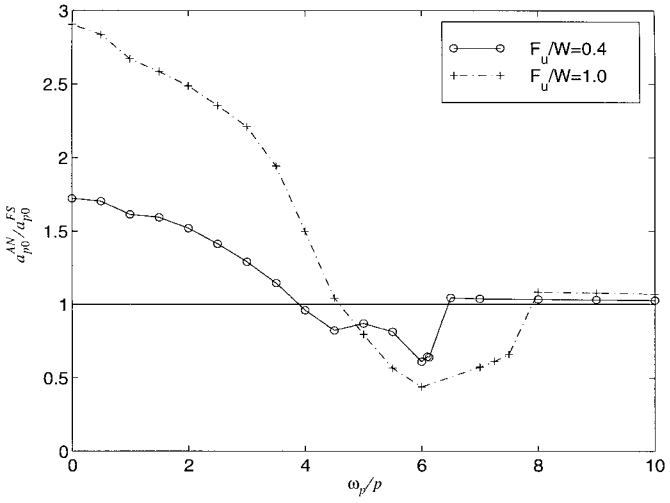

FIG. 10. Normalized Minimum Overturning Acceleration Levels Needed to Overturn Anchored Block (Elastic-Plastic Behavior, $\mu = 5$) to Acceleration Level Needed to Overturn Same Block When It Is Free Standing

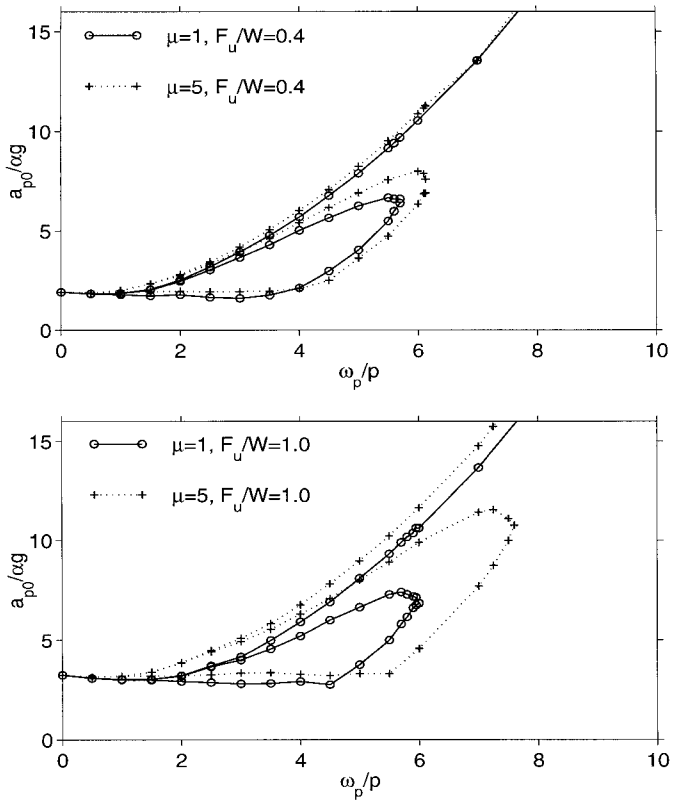

FIG. 11. Comparison of Overturning Acceleration Spectra Computed with Nonlinear Formulation for Anchored Block ($\alpha = 0.349$ rad = 20°, $p = 2$ rad/s, $\eta = 0.825$, $q = 5.2 \times 10^{-4}$) with Two Levels of Ductility: $\mu = 1$ and 5 (Top: $F_u/W = 0.4$; Bottom: $F_u/W = 1.0$)

ROCKING RESPONSE OF ANCHORED BLOCKS UNDER EARTHQUAKE EXCITATIONS

The foregoing analysis revealed that under a one-sine (Type-A) pulse there are two modes of overturning. The presence of restrainers is more effective for low-frequency pulses or small

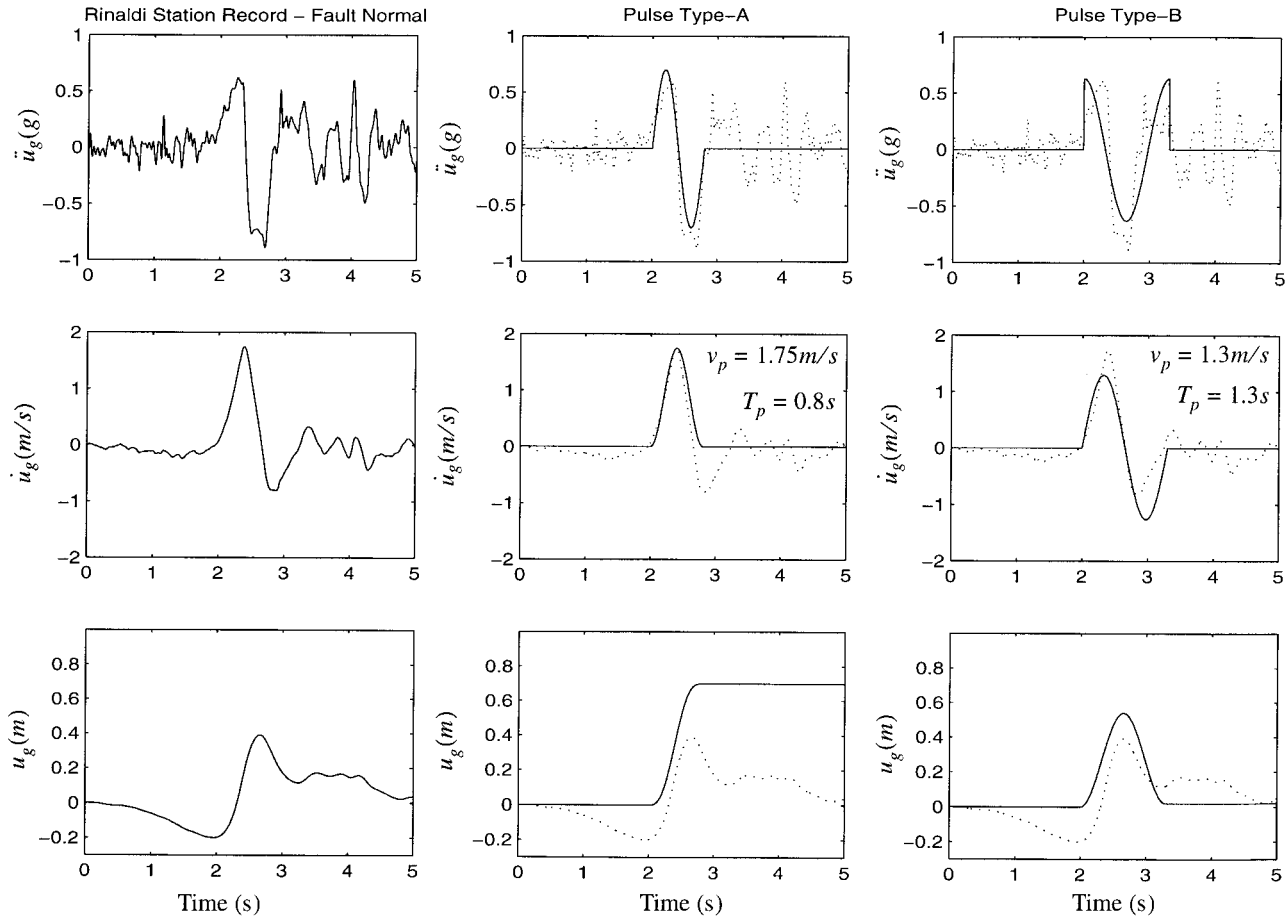

FIG. 12. Fault-Normal Components of Acceleration, Velocity, and Displacement Time Histories Recorded at Rinaldi Station during January 17, 1994, Northridge, Calif., Earthquake (Left); Cycloidal Type-A Pulse (Center); Cycloidal Type-B Pulse (Right)

blocks. As the size of the block or the frequency of the pulse increases, the presence of restrainers is destructive because anchored blocks overturn under acceleration amplitudes smaller than those needed to overturn free-standing blocks. For large values of ω_p/p, blocks overturn only along mode 2 (no impact) and the effect of the restrainers is marginal.

In this section the seismic response of anchored blocks subjected to selected strong ground motions is presented. Fig. 12 (left) portrays the fault-normal component of the acceleration, velocity, and displacement histories of the January 17, 1994, Northridge, Calif., earthquake recorded at the Rinaldi station. This motion resulted in a forward ground displacement that recovered partially. The velocity history has a large positive pulse and a smaller negative pulse that is responsible for the partial recovery of the ground displacement. Had the negative velocity pulse generated the same area as the positive velocity pulse, the ground displacement would have fully recovered. Accordingly, the fault-normal component of the Rinaldi station record is in between a forward and a forward-and-back pulse. Fig. 12 (center) plots the acceleration, velocity, and displacement histories of a Type-A cycloidal pulse. The forward ground displacement is expressed by (Jacobsen and Ayre 1958; Makris 1997)

$$u_g(\tau) = \frac{v_p}{2}\tau - \frac{v_p}{2\omega_p}\sin(\omega_p\tau), \quad 0 \le \tau \le T_p \tag{51}$$

whereas the ground velocity and ground acceleration are expressed by the time derivatives of (51). In constructing Fig. 12 (center), one assumes a pulse duration $T_p = 0.8$ s and a velocity amplitude $v_p = 1.75$ m/s, which are approximations of the duration and velocity amplitude of the first main pulse shown in the record. This comparison indicates that the simple one-sine pulse, which was used in this study to uncover the many complexities of the rocking response of a rigid block, can approximate the kinematic characteristics of some recorded ground motions. Fig. 12 (right) plots the acceleration, velocity, and displacement histories of a Type-B cycloidal pulse. The forward-and-back ground displacement is expressed by (Makris 1997; Makris and Roussos 1998)

$$u_g(\tau) = \frac{v_p}{\omega_p} - \frac{v_p}{\omega_p}\cos(\omega_p\tau), \quad 0 \le \tau \le T_p \tag{52}$$

In constructing Fig. 12 (right), one assumed a pulse duration $T_p = 1.3$ s and a velocity amplitude $v_p = 1.3$ m/s.

The analysis proceeds by computing the rocking response of a larger block (1.0 × 3.0 m), which has a frequency parameter $p = 1.525$ rad/s and slenderness $\alpha = 18.43°$. Under the assumption that the Rinaldi station record can be approximated with a one-sine pulse with $T_p = 0.8$ s, the corresponding frequency ratio is $\omega_p/p = 5.15$. For this value of the frequency ratio, Fig. 9 (which has been generated for a smaller, less slender block; $\alpha = 20°$, $p = 2$ rad/s, and $\eta = 0.825$) indicates that a free-standing block might survive a stronger acceleration level than an anchored block. Indeed Fig. 13 indicates that the 1.0 × 3.0 m free-standing block overturns at a 127% level of the Rinaldi record, whereas the same block anchored with restrainers having strength $F_u = 0.4W$ and ductility $\mu = 5$ overturns under only a 119% level of the Rinaldi acceleration record, as shown in Fig. 14. This puzzling result partly motivated the study reported herein, which addressed the rocking problem of anchored blocks in a systematic and lucid manner.

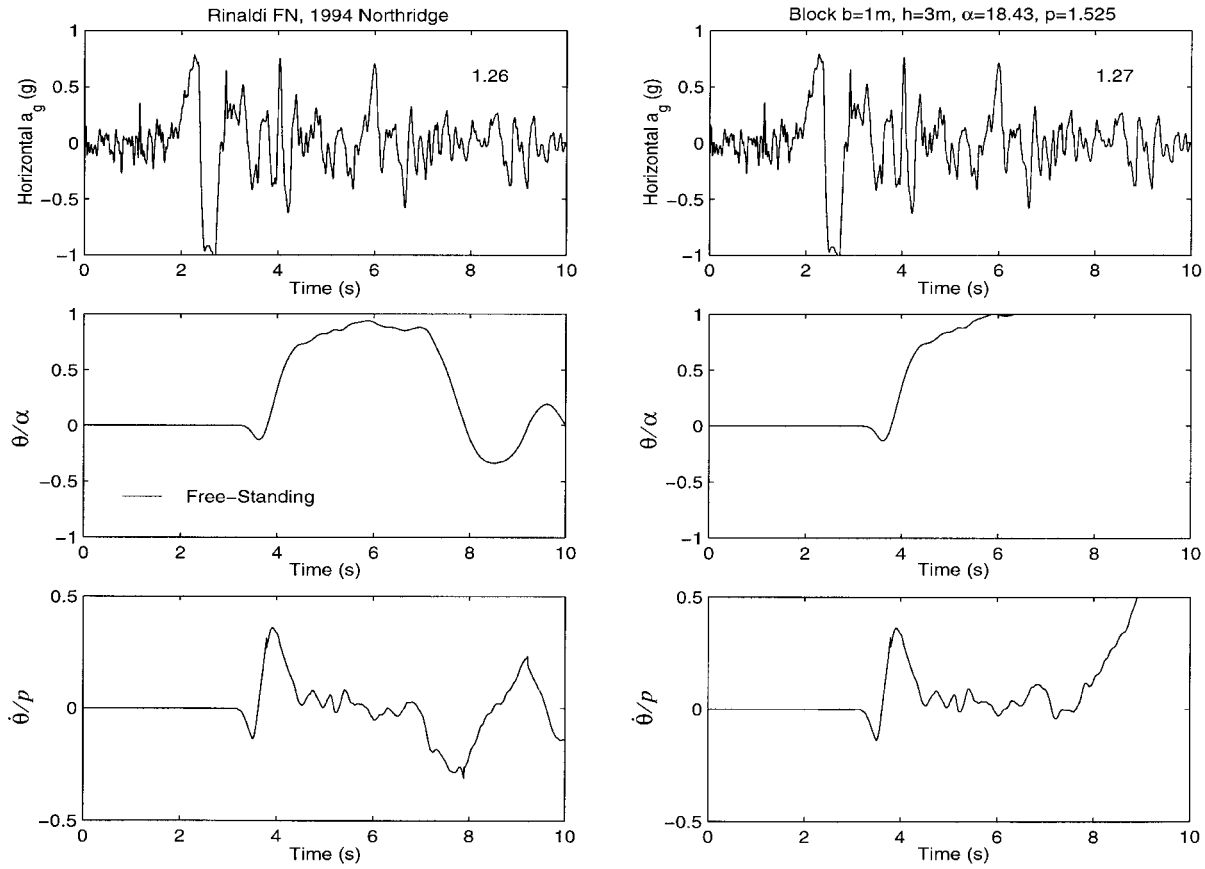

FIG. 13. Rotation and Angular Velocity Time Histories of Free-Standing Block (b = 1.0 m, h = 3.0 m) Subjected to Fault-Normal Rinaldi Station Motion [Left: No Overturning (126% Acceleration Level); Right: Overturning (127% Acceleration Level)]

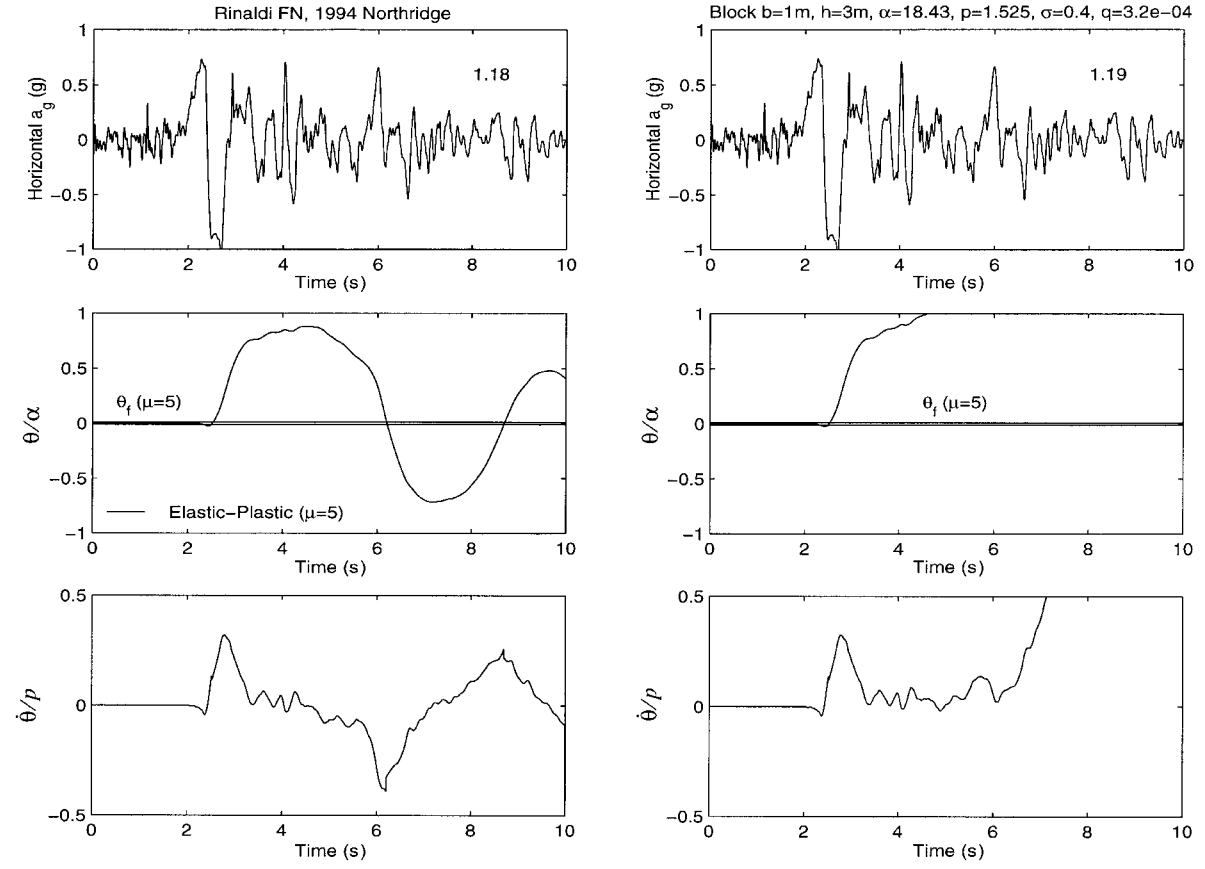

FIG. 14. Rotation and Angular Velocity Time Histories of Larger Anchored Block (b = 1.0 m, h = 3.0 m, F_u/W = 0.4, and μ = 5) Subjected to Fault-Normal Rinaldi Station Motion [Left: No Overturning (118% Acceleration Level); Right: Overturning (119% Acceleration Level)—Free-Standing Block Can Survive Stronger Acceleration Level Than Anchored Block (Fig. 13)]

CONCLUSIONS

This paper investigates the transient rocking response of anchored electrical equipment and other tall structures that can be approximated as rigid blocks. Restrainers and elastic-brittle and elastic-plastic behavior are considered. It is found that restrainers are more efficient in preventing overturning of small slender blocks subjected to a low-frequency ground excitation. Under a one-sine pulse, anchored blocks can overturn with two distinct modes of overturning: (1) by exhibiting one impact; and (2) without exhibiting any impact. Along the frequency spectrum, just prior to the transition from mode 1 to mode 2, the presence of restrainers has a destructive effect. The stronger the restrainer, the smaller is the acceleration amplitude needed to overturn an anchored block, whereas a free-standing block can withstand the higher acceleration amplitude. This counterintuitive response extends when the restrainers exhibit finite ductility, because the study shows that there is a frequency range where blocks with the most ductile restrainers will withstand the smaller acceleration level. Larger blocks can overturn only without experiencing any impact (mode 2), and in this case, the effect of restrainers is marginal even when their strength equals the weight of the rocking block. The limited effect of restrainers in preventing toppling is also found under earthquake excitations. The study shows that, under the Rinaldi station record, restrainers with strength $F_u/W = 0.4$ and ductility $\mu = 5$ have a destructive effect in preventing toppling of a 1.0×3.0 m block, because when the block is free standing it survives the level of motion that overturns it when it is anchored.

ACKNOWLEDGMENTS

This work is supported by the Pacific Gas and Electric Company under Grant PG&E-UCB-00956 to the Pacific Earthquake Engineering Center, University of California, Berkeley, Calif.

REFERENCES

Bouc, R. (1971). ''Modele mathematique d'hysteresis.'' *Acustica*, 24, 16–25 (in French).

Dimentberg, M. F., Lin, Y. K., and Zhang, R. (1993). ''Toppling of computer-type equipment under base excitation.'' *J. Engrg. Mech.*, ASCE, 119(1), 145–160.

Jacobsen, L. S., and Ayre, R. S. (1958). *Engineering vibrations*, McGraw-Hill, New York.

Makris, N. (1997). ''Rigidity-plasticity-viscosity: Can electrorheological dampers protect base-isolated structures from near-source ground motions?'' *Earthquake Engrg. and Struct. Dyn.*, 26, 571–591.

Makris, N., and Roussos, Y. (1998). ''Rocking response and overturning of equipment under horizontal pulse-type motions.'' *Rep. No. PEER-98/05*, Pacific Earthquake Engineering Research Center, University of California, Berkeley, Calif.

Milne, J. (1885). ''Seismic experiments.'' *Trans. Seism. Soc. Japan*, 8, 1–82.

Wen, Y.K. (1975). ''Approximate method for nonlinear random vibration.'' *J. Engrg. Mech. Div.*, ASCE, 101(4), 389–401.

Wen, Y.K. (1976). ''Method for random vibration of hysteretic systems.'' *J. Engrg. Mech. Div.*, ASCE, 102(2), 249–263.

Zhang, J., and Makris, N. (2001). ''Rocking response of free-standing blocks under cycloidal pulses.'' *J. Engrg. Mech.*, ASCE, 127(5), 473–483.